Photometry of 10 Million Stars from the First Two Years of TESS Full Frame Images - Part II

Chelsea X. Huang,[1, *] Andrew Vanderburg,[2] Andras Pál,[1] Lizhou Sha,[1, 2] Liang Yu,[1] Willie Fong,[1] Michael Fausnaugh,[1] Avi Shporer,[1] Natalia Guerrero,[1] Roland Vanderspek,[1] and George Ricker[1]

[1]*Kavli Institute for Astrophysics and Space Research, MIT*
[2]*Department of Astronomy, University of Wisconsin-Madison*

(Revised November 12, 2020)

ABSTRACT

We present light curves from a magnitude limited set of stars and other stationary luminous objects from the TESS Full Frame Images, as reduced by the MIT Quick Look Pipeline (QLP). Our light curves cover the full two-year TESS Primary Mission and include $\sim 14,770,000$ and $\sim 9,600,000$ individual light curve segments in the Southern and Northern ecliptic hemispheres, respectively. We describe the detrending techniques we used to create the light curves, and compare the noise properties with theoretical expectations. All of the QLP light curves are available at MAST as a High Level Science Product (HLSP) via 10.17909/t9-r086-e880[a)]. This is the largest collection of TESS photometry available to the public to date.

Keywords: TESS — survey — pipeline

INTRODUCTION

The Transiting Exoplanet Survey Satellite (TESS) mission (Ricker et al. 2015) presents an enormous opportunity to study the precise time series of tens of millions of bright stars in the entire sky. Using its 30 min cadence Full Frame Images (FFIs), we have extracted photometry for a magnitude limited set of stars and other stationary luminous objects observed by TESS in the first two years. The TESS FFI photometry technique by the MIT Quick Look Pipeline (QLP) are presented in a previous article (Huang et al. 2020). Here, we describe how the QLP postprocesses its light curves and evaluate the pipeline's performance in terms of photometric precision. We also discuss some caveats of our data products that users should keep in mind while working with QLP light curves. We publicly release QLP light curves for all sources in the TESS Input Catalog (TIC, Stassun et al. 2018, 2019) observed by TESS in its primary mission down to a limiting TESS magnitude T of 13.5. We also added in stars with proper motion larger than 200 mas yr^{-1} and brightness between TESS Magnitude 13.5 and 15 (most of which are nearby M-dwarfs).

LIGHT CURVE POST-PROCESSING

We start with the light curves extracted by the QLP from the TESS FFIs, as described in Part I; we call this the "raw light curve". The raw light curve from the best aperture is available in the FITS file of QLP HLSP product on MAST under keywords **SAP_FLUX**.

TESS light curves usually contain low-frequency variability from stellar activity or instrumental noise, which must be filtered before the small, short-duration signals caused by transiting planets can be detected. We detrend the light curves by applying a high-pass filter before they are searched for transits. Before detrending, we reject outliers in the light curve using the quaternion time series [1]. Any exposure corresponding to abnormal amplitudes of scatter in the quaternion time series is not used for detrending. We then fit the light curves from each spacecraft orbit with

[a)] https://archive.stsci.edu/hlsp/qlp

[*] Torres Postdoctoral Fellow

[1] The quaternion series can be downloaded from https://archive.stsci.edu/missions/tess/engineering/. See Vanderburg et al. (2019) for more details, although note that QLP does not use decorrelate the light curves against the quaternion time series as done by Vanderburg et al. (2019)
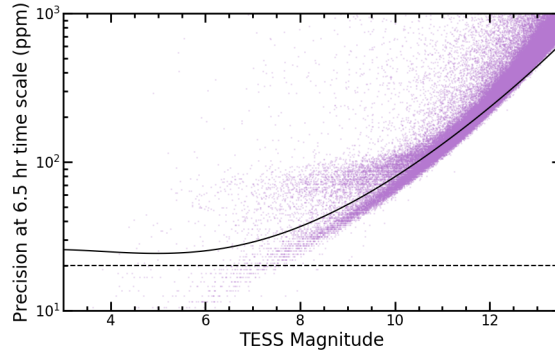
Figure 1. Right: The photometric precision of the time series, compared to expected theoretical precision estimated in Sullivan et al. (2015) (solid line). The dashed horizontal line is a reference indicating 20 ppm precision.

a basis spline (Vanderburg & Johnson 2014; Shallue & Vanderburg 2018; Vanderburg et al. 2019). We choose the spacing of the spline break points by minimizing the BIC, imposing a minimum allowed spacing of 0.3 days. This minimum spacing is optimized for the detection of planets with short orbital periods, which may lead to the distortion of long-duration transits. We provided flattened light curves from three apertures with different sizes. The light curve from the best aperture is under FITS keyword **KSPSAP_FLUX**. The light curve from the relatively bigger/smaller apertures are under FITS keyword **KSPSAP_FLUX_LAG** and **KSPSAP_FLUX_SML**, respectively.

After detrending, we identify anomalous exposures in the light curves. For each exposure, we look at the set of stars with TESS magnitude between 9.5 and 10 and calculate the fraction which exhibit photometric precision more than 75% worse than the pre-flight anticipated photometric precision of 200 parts per million (ppm) per hour for stars with $T = 10$ mag. If more than 20% of the stars observed on the same CCD have poor precision at a particular exposure, we assign a bad quality flag to the corresponding exposure. This flag is stored as bit 13 in the **QUALITY** column provided in the light curve products. The rest of the bits are adopted from the SPOC Full Frame Image headers (Jenkins 2015; Jenkins et al. 2016).

We combine the detrended light curves observed in two TESS orbits of each TESS sector by offsetting the median of the light curves to the expected TESS magnitude, after rejecting bad-quality points. These magnitude time series are then converted to normalized flux time series in the final light curve products.

The QLP produces light curves of each source from up to five apertures. We identify an optimal light curve for each target based on the source's brightness. Early in the mission, we calculated the photometric precision in each aperture for a set of stars and determined the aperture size that yielded the best photometric precision as a function of TESS-band magnitude in 13 evenly spaced bins between TESS mag of 6 to 13.5, and used those results to select the optimal aperture.

We show the precision of our light curves in Figure 1. For comparison, the solid line is the theoretical photometric precision estimated by Sullivan et al. (2015) scaled to a 6.5 hr time scale, assuming Gaussian noise. The photometric precision roughly follows the prediction for the majority of the stars and has a lower noise floor (approximately 20 ppm) for the brightest stars [2].

CAVEATS

QLP light curve production depends critically on the *TESS* band magnitudes estimated by the TESS Input Catalog (TIC, Stassun et al. 2018, 2019). If a star's *TESS* band magnitude is incorrect, the amplitude of features in the QLP light curve will be likewise incorrect because the QLP will deblend the light curve incorrectly. The uncertainties of the amplitude of variations in the flux time series therefore depend on the uncertainties in the TESS magnitudes. This is not represented in the error bars we provide in the light curve time series. Instead, the uncertainties are estimated with the Median Absolute Deviation statistics of each orbit of light curves multiplied by 1.4826.

We note that light curves from Sectors 1–13 were produced using TIC 7, while light curves in Sector 14 onward were produced using TIC 8. A small fraction of stars have different estimated *TESS* magnitudes in TIC 7 versus TIC 8.

---

[2] The in-orbit performance of the TESS photometers is better than preflight calculations by Sullivan et al. (2015), which has been traced to an underestimation in their assumed telescope aperture.

These changes in magnitude affect the amount of deblending applied by QLP and thus the amplitude of light curve features.

Our method of deblending the light curve time series also do not take into account that the target stars' point spread functions may be not fully contained in the smallest circular aperture (with a radius of 1.75 pixel), leading to underestimation of signal amplitudes in this particular aperture for some stars.

The TICA software we used to calibrate the TESS raw FFIs went through many iterations during the TESS Primary Mission. We did not keep a record of the particular versions of the calibration software used for each sector of data. For a fraction of the sectors, the TICA smear correction estimate lead to column contamination in the light curves of a small number of stars. Users can examine light curves of stars located in the same column to identify such contamination. We expect this issue to be resolved with future data reprocessing and releases.

Software: Golang (Meyerson 2014), Astropy (Astropy Collaboration et al. 2013; Price-Whelan et al. 2018)

REFERENCES

Astropy Collaboration, et al. 2013, A&A, 558, A33,
    doi: 10.1051/0004-6361/201322068

Meyerson, J. 2014, IEEE software, 31, 104

Huang, C. X., et al., RNAAS in press

Jenkins, J. M. 2015, in AAS/Division for Extreme Solar
    Systems Abstracts, Vol. 3, AAS/Division for Extreme
    Solar Systems Abstracts, 106.05

Jenkins, J. M., et al. 2016, Society of Photo-Optical
    Instrumentation Engineers (SPIE) Conference Series,
    Vol. 9913, The TESS science processing operations
    center, 99133E

Price-Whelan, A. M., et al. 2018, AJ, 156, 123,
    doi: 10.3847/1538-3881/aabc4f

Ricker, G. R., et al. 2015, Journal of Astronomical
    Telescopes, Instruments, and Systems, 1, 014003.
    doi:10.1117/1.JATIS.1.1.014003

Shallue, C. J., & Vanderburg, A. 2018, AJ, 155, 94,
    doi: 10.3847/1538-3881/aa9e09

Stassun, K. G., et al. 2018, AJ, 156, 102,
    doi: 10.3847/1538-3881/aad050

Stassun, K. G., et al. 2019, AJ, 158, 138,
    doi: 10.3847/1538-3881/ab3467

Sullivan, P. W.,et al. 2015, ApJ, 809, 77,
    doi: 10.1088/0004-637X/809/1/77

Vanderburg, A., & Johnson, J. A. 2014, PASP, 126, 948,
    doi: 10.1086/678764

Vanderburg, A., et al. 2019, ApJL, 881, L19,
    doi: 10.3847/2041-8213/ab322d